Unsteady nodal modeling of building ventilation networks

Ali Esber, Xavier Faure, Francois Demouge, Etienne Wurtz, Simon Rouchier

Building and Environment 209 (2022) 108671

Contents lists available at ScienceDirect

Building and Environment

journal homepage: www.elsevier.com/locate/buildenv

Unsteady nodal modeling of building ventilation networks

Ali Esber [a,b,c,*], Xavier Faure [a], François Demouge [c], Etienne Wurtz [a], Simon Rouchier [b]

[a] Univ. Grenoble Alpes, CEA, Liten, Campus Ines, 73375, Le Bourget du Lac, France
[b] Université Savoie Mont-Blanc, CNRS, LOCIE, 73000, Chambéry, France
[c] Scientific and Technical Center for Building, CSTB, France

ARTICLE INFO

Keywords:
Concept of quasi-staticity
Ventilation system
Wind turbulence
Pressure fluctuation
Internal resonance

ABSTRACT

Ventilation network design and analysis are generally performed using nodal approaches (egg. 1 node for each zone) and quasi-static assumption. Thus, inertia effects of ducts are neglected as well as any possible acoustic resonance that could occur in any internal volume. These effects might be not as negligible as one could think while studying particular transient boundary conditions. Wind effect, including its turbulence, even at relatively small velocity, windstorm impact, flow disturbance, imply internal pressure fluctuations that cannot be caught if quasi-static assumption is considered within nodal numerical models. Inertia effect is not automatically linked to compressible and resonance assumptions can be identified even in incompressible conditions.

The present study aims to identify in which cases the quasi-static assumption can be made. Simple stepwise boundary conditions are applied on a simple configuration with one zone and two ducts. The MATHIS software, developed to analyze ventilation systems in buildings and chosen as the standard tool in the French context, is used for this study and validated under unsteady state for a single zone case. A new approach is proposed to build a unique graphical analysis from two groups of terms, being define using a dimensionless method. Its usage enables to highlight in which situation internal pressure resonance will happen and therefore helps the modeler to choose the correct assumptions for further simulations.

1. Introduction

Steered by the global energy consumption's concern in the construction sector, building's standards and codes have tremendously increased their requirements worldwide. Concerning the heating needs, code's thresholds have decreased between 40% and 80% since 1975 in different countries. Several thresholds for maximum envelope U-values, maximum envelope airtightness, minimum window to wall surface ratio, can be seen in different standards for the building itself. In addition, thresholds on the energy consumption and indoor ambiance (for potential cooling needs or summer comfort) are applied later on the operation side of the building, using predefined schedules of occupancy and specific weather conditions for the built area and validated simulation tools. To target the final energy policies, each country applies several energy conversion factors for the different energy carriers used by the building's designer.

Aside from the energy requirement, indoor comfort and air quality raised in interest and concern during the design process. The coupling of energy, indoor air quality and thermal comfort concerns, further steered by the energy targets, led to raise the importance of ventilation systems. Envelope air tightness improvements made mandatory in the different building's code, lowered down the resilience of fully exhaust ventilation systems [1]. As the airflow paths within the envelope was reduced, the global airflow network became sensitive to the envelope leakage's distribution. Therefore, the simulations coupling heat and mass transfer are increasingly used during the early design stage in order to ensure the compliance of energy and indoor air quality requirements.

Nowadays, the ventilation system's design stages are performed using simulation tools based on a nodal approach coupling heat and mass transfer. The nodal approach is based on mixed assumptions in each zone of the building. The mass transfer balance is computed using links between zones, defined by airflow paths based on Bernoulli's assumption. In order to preserve some reasonable computation time, the quasi-static assumption is generally applied for the mass balance which leads to neglect any possible resonance of internal pressure. But while conducting resilience analyses of ventilation systems, particular transient boundary conditions must be considered. Wind turbulence and windstorm on any building or accidents such as vacuum vessels bursting in industrial buildings, could occur. To the authors' knowledge, very few

* Corresponding author. Univ. Grenoble Alpes, CEA, Liten, Campus Ines, 73375, Le Bourget du Lac, France.
E-mail addresses: Ali.esber@cea.fr, Ali_esber93@hotmail.com (A. Esber), Xavier.faure@cea.fr (X. Faure), Francois.demouge@cstb.fr (F. Demouge), Etienne.wurtz@cea.fr (E. Wurtz), Simon.rouchier@univ-smb.fr (S. Rouchier).

https://doi.org/10.1016/j.buildenv.2021.108671
Received 30 September 2021; Received in revised form 30 November 2021; Accepted 7 December 2021
Available online 10 December 2021

Nomenclature

variables	units Description
P	Pa Thermodynamic pressure
P_{atm}	Pa Atmospheric pressure
t	s time
C_p	$J.kg^{-1}.K^{-1}$ Specific heat at constant pressure
C_v	$J.kg^{-1}.K^{-1}$ Specific heat at constant volume
z	m Elevation from node's altitude
Z_a	m Node altitude from reference point
V	m^3 volume
$\dot{E}$	w Net heat flux
$\dot{m}$	$kg.s^{-1}$ Net mass flux rate
ρ	$kg.m^{-3}$ density
T	K temperature
Y_k	$Kg.Kg^{-1}$ Mass fraction of K^{th} specie
L	m length
g	$m.s^{-2}$ Gravity
Q	$m^3.s^{-1}$ Volumetric flow rate
S	m^2 area
R	m^{-4} Resistance aeraulic
U	$m.s^{-1}$ velocity
f	Hz frequency
M	$kg.mol^{-1}$ Molar mass

studies were found related to the subject of internal pressure fluctuation due to sudden variations in the boundary conditions. The major study, a fundamental physics-based approach, was published by Holmes in 1979 [2]. Holmes studied analytically and experimentally the influence of a pulsed flow on an enclosure volume with a single opening. Pulsed flow is defined by a change in the external pressure at the opening, causing fluctuating flow inside the enclosure due to the compressibility of the air in the enclosure [3]. Holmes [2] then defines the first reliable model to study resonance and internal fluctuations, when these fluctuations were not properly taken into account as external fluctuations. Regarding natural ventilation, several studies have been found using the dimensionless ratios to consider for conducting reduced scale experiments [4–10] and especially the volume distortion resulting from dimensionless analyses between length and velocity scales respectively. Within these, Etheridge (2000a and 2000b) [9,10] proposed an analytical approach for buildings submitted to wind turbulence, including quasi-static and compressibility impact on the internal pressure response to external solicitation. For the studied cases, inertia had a greater effect compared to air compressibility. For mechanical ventilated buildings, very few studies have been found with analytical development of instantaneous flow and conditions for internal pressure resonance effect. Concerning residential buildings, the only reported study found was concerning a demand-response exhaust ventilation system by Monajed (1989) [11]. Even though no quantitative results were given, these effects of internal pressure fluctuation were still discussed. Monajed [11] presented several points to be pursued, such as the knowledge of the distribution of pressure coefficients as well as the behavior of openings. He insisted on the global experimental validation of the physical models used for air transfer through openings. Finally, he suggested that new research should take into account some phenomena which, until recently, were either considered as negligible or modeled in a simplified way (like the spatio-temporal fluctuations of the wind). Lastly, for industrial nuclear plants, LeRoux (2011), in his PhD [12] studied mean [13] and transient [14] airflow in complex ventilation systems under different conditions, including windstorm and guard mode of operation for the ventilation system.

Disturbance of the negative pressure cascade among the different zones was analyzed for specific transient boundary conditions. Reduced-scale wind tunnel experiments and numerical simulations were considered. LeRoux mentioned the importance of the branch and volume inertia in internal pressure fluctuation, but these had negligible impacts in his study due to the global constraints of the considered ventilation plant.

From the related studies found in the literature, there is still a lack of knowledge of the conditions in which quasi-static assumption remains true. Simulating such events of highly variable boundary conditions, for any kind of building, requires checking the veracity of the quasi-static assumption. From the author's knowledge, no study has addressed this effect in a more generic view. This study aims to highlight the range of applicability of the quasi-static assumption in a dimensionless form. It is steered by the will of studying the impact of wind turbulence on the resilience of ventilation systems. Therefore, the very first assumption of quasi-staticity needs to be carefully analyzed as a first step toward the above-mentioned aim.

This requires creating a methodology to allow the development of new approaches to study the aeraulic behavior of ventilation networks for permanent and transient flows. This study uses the MATHIS open-source software [15], developed by the French Scientific and Technical Center For Building (CSTB), for ventilation systems design in residential buildings. MATHIS consists of a numerical nodal modeling approach including the coupling between air flows, temperature, and pollutants. It is already validated, compared to experimental data from wind tunnel experiments [16], for the mass balance model and the BESTEST process for the energy balance model [17].

The simple configuration considered in the study is presented below. It is the same case used in Ref. [14]. Therefore, results from MATHIS are validated for several parameters and resonance observations in the internal volume. Some discussions are proposed from these first results and followed by several simulations of practical examples on different cases and types of buildings.

In order to cover any kind of building, a dimensionless approach is proposed afterward and the same results for all presented cases are then presented in one single graph with two main groups of variables derived from the dimensionless method. Finally, a conclusion is drawn.

2. Configuration of analysis

This study considers a simple case which consists of a single zone connected with ducts for inlet and outlet respectively (Fig. 1). It is the same case presented in Ref. [14] which results are used for MATHIS' validation. The configuration consists in a single volume (V in m^3) with two airflow paths defined by their length (m), their crossed-section (m2) and their internal resistance R (m^{-4}). Each parameter is changed in order to represent different cases and identify in which conditions internal pressure resonance can occur. As shown in the following, this simple configuration enables to study how internal pressure resonance can occur depending on the geometric characteristics of either the volume and both ducts and inlet boundary conditions.

The referenced results, used for validation, come from Ref. [14] who made similar simulations using both a self-made model and SYLVIA, a

Fig. 1. Simulation zone.

nodal software designed for nuclear plant ventilation systems [18]. [14] also provides experimental results using a specifically designed test bed for the sake of its own validation.

Specific boundary conditions are applied for all simulations, consisting of a pressure step on one side and leaving constant the other airflow path's output pressure condition. As shown in Fig. 2, an instantaneous pressure step of 2000 Pa, is imposed to the inlet duct of the room in order to study its propagation within the case presented in Fig. 1. The time step of all simulations is 0.005 s as for [14]. The simulation ends when a stationary regime is finally met.

Results are analyzed through the internal pressure fluctuation signal and several characteristics are computed. As shown in Fig. 3, four indicators are defined:

- The oscillation's frequency (in Hz)
- The time needed to reach the established regime within 5% of margin (Tr 5% in s)
- The time to firstly reach 90% of the established regime (Tm in s)
- The percentage of the first overshot (D1 in %).

The latter is computed taking the established pressure value as the reference. If no pressure fluctuation is observed, the above-mentioned indicators are not computed. The frequency is computed only if a full period, starting with the first overshot, is observed with oscillations of at least 1% of the established regime.

The validation consists of performing the same simulations as in Ref. [14] and over-plotting the indicators presented above. MATHIS validation is presented in the following section.

3. MATHIS' validation

MATHIS is a nodal numerical model coupling heat and mass transfer. In each node i that represents a volume, the conservation of mass, internal energy and species' mass fraction are applied through equations (1)–(3) respectively.

$$\frac{dP^i}{dt} = \frac{C_P^i/C_V^i - 1}{V^i}\left(\dot{E}^i\right) + \rho^i T^i \sum_k \left(C_{Pk}^i - \frac{C_P^i}{C_V^i} C_{Vk}^i\right) \frac{dY_k^i}{dt} \tag{1}$$

$$\frac{dT^i}{dt} = -\frac{T^i}{\rho^i V^i}\left(\dot{m}^i\right) + \frac{1}{\rho^i V^i C_V^i}\left(\dot{E}^i\right) - \frac{T^i}{C_V^i}\sum_k C_{Vk}^i \frac{dY_k^i}{dt} \tag{2}$$

$$\frac{dY_k^i}{dt} = \frac{1}{\rho^i V^i}\left(\dot{m}_k^i - Y_k^i \dot{m}^i\right) \tag{3}$$

It uses to constant gas relationship in equation (4) enabling to close the systems and compute the air density.

$$\rho^i = \frac{P^i}{T^i\left(C_P^i - C_V^i\right)} \tag{4}$$

In each branch or airflow path that links either the zones to each other or to boundary conditions, stated by i and j for the two sides of the path, the mechanical energy conservation is applied using equation (5).

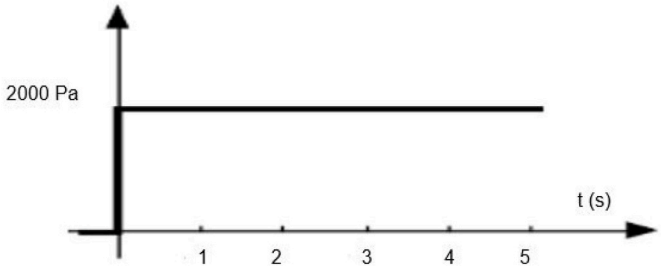

Fig. 2. Pressure step of 2000 Pa.

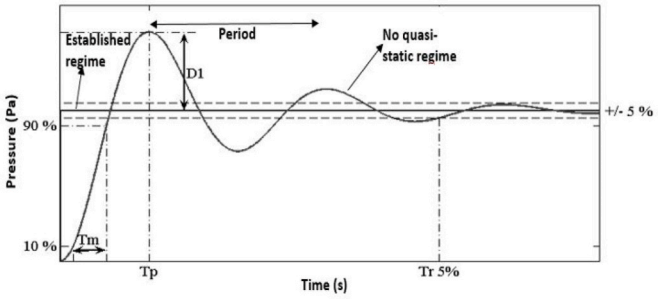

Fig. 3. Different characteristics to analyze a Signal: Time response at 90% (Tm in s), Overshoot D1 (%), Frequency (1/Period in Hz) and Established time response (Tr 5% in s: time needed to be within 5% of the established pressure value).

It is based on the generalized Bernoulli's equation.

$$\frac{Ld\dot{m}}{Sdt} = \left(P_i - \rho_i g z_i\right) - \left(P_j - \rho_j g z_j\right) + \rho g\left[\left(z_{ai} + z_i\right) - \left(z_{aj} + z_j\right).\right] + \Delta P_{loss} \tag{5}$$

with ΔP_{loss} the pressure drops for the specific airflow path represented. In this study, the duct losses are assumed to be quadratic, thus leading to $\Delta P_{loss} = R\rho(Q)^2$, with R being the aeraulic resistance used further in parametric simulations.

It is important to clearly define the impact of either isothermal, quasi-static, constant specific heat or incompressible assumptions:

- Isothermal assumption leads to compute dynamically a source/sink of heat to compensate the temperature variation in equation (2) at each time step.
- Quasi-static assumption leads to neglect the left-hand side term in equations (1) and (5).
- Constant specific heat assumption leads to neglect the right-hand end term in equations (1) and (2).
- Incompressible assumption leads to take the atmospheric pressure instead of the zone's one, $P^i = P_{atm}$ one, in equation (4).

In the following, the isothermal assumption is used. Except special mention, the incompressible assumption is also considered, but its impact is studied further. As no specific species is considered in the study, the constant specific heat assumption is tacitly true in the system and equation (3) is not considered.

In order to validate MATHIS, a comparison procedure is carried out between the results of [14] and the results of MATHIS using the above-described case. The model of [14] has been rebuilt for the purpose of this validation. It consists of three differential equations. Two are derived from the energy balance in the two ducts and one from the mass conservation in the internal volume. The three equations (6)–(8) are presented in a dimensionless form in system [14].

$$\frac{\rho_i^* L_i^*}{S_i^*}\frac{dQ_i^*}{dt^*} = P_i^* - P_v^* - \left(R_{ref} S_{ref}^2\right)\rho_i^* R_i^* Q_i^{*2} \tag{6}$$

$$\frac{\rho_v^* L_o^*}{S_o^*}\frac{dQ_o^*}{dt^*} = P_v^* - P_o^* - \left(R_{ref} S_{ref}^2\right)\rho_v^* R_o^* Q_o^{*2} \tag{7}$$

$$\frac{dP_v^*}{dt^*} = \left(\frac{P_{atm} S_{ref} L_{ref}}{\rho_{ref} U_{ref}^2 V_{ref}}\right)\left(\frac{\rho_i^* Q_i^* + \rho_0^* Q_o^*}{V_v^*}\right) \tag{8}$$

With subscript *i* standing for *inlet*, *o* for *outlet*, and *v* for *volume*. The upper scripts * stand for dimensionless variable. Referenced values (subscript *ref*) are taken in accordance with [14]. This system is introduced further as the basis of the dimensionless approach.

The model is used to run parametric simulations with the aeraulic

resistance varying from 10 to 100,000 (one step per decade) and the lengths from 1 to 100 m in 4 steps (1, 10, 50 and 100). With the step changes of the resistance and the length of the airflow paths, a total number of combinations of 148 (4 × 37) is obtained. All combinations have been simulated, but only the one leading to internal pressure resonance are considered for further analyses with computing the four previously described indicators. A signal with at least one overshoot above 5% is considered as having a resonance effect.

Fig. 4 represents the four indicators, i.e., frequency, overshot %, time response at 5% and rising time for the different values of aeraulic resistance. Each series of point represent a duct length. Reference case is presented by filled circles and MATHIS results non-filled circle. Fig. 4 shows that results from MATHIS match with the results of [14] and thus validate the capability of MATHIS to reproduce internal pressure fluctuations in incompressible and isothermal conditions.

From Fig. 4, one can notice first that inertia (through the duct's length) and aeraulic resistance have both a high effect on internal fluctuation. The airflow path's resistance work like a damper that reduces the value of the internal pressure fluctuation. As shown from the upper left figure of Fig. 4, the lower the resistance and the inertia, the higher the frequency Depending on the amount of inertia, some thresholds in the resistance are systematically present and for which above any possible internal pressure oscillation is observed. Internal resonance's frequency increases for a combination of lower resistance and lower inertia. But the resistance's threshold, for under which resonance occurs, increases as the inertia increases. Indeed, with duct length of 1 m, and thus small inertia, no resonance is observed for duct's resistance of 5 m^{-4} and above, while for duct length of 100 m, resonance occur up to resistance of 5000 m^{-4}. The time response to reach the established regime within 5% of margin logically increases for higher inertias with low resistances, this time response follows the times response at 90% above the resistance's threshold. The overshoot observation shows an increasing amplitude, up to 100% of the established pressure value for the low resistance's values, as the inertia increases.

As shown previously, some internal pressure resonances can occur, these are led mainly by the branch inertia rather than the compressibility of the flow. As also presented in Ref. [10], the impact of compressibility of air is not to change the above results. The same simulations were realized considering the air compressibility and the same indicators were computed. As shown in Fig. 5, both incompressible and compressible results give the same results for internal pressure resonance's observations and same values for the four indicators computed from now for the comparison. As a reminder, the differences between incompressible and compressible rely on the density being dependent only on the atmospheric pressure or local pressure respectively (see equation (4)).

The cases studied in the following steps will be incompressible in order to reduce the number of equations related to the density variation. Besides, all cases are also run under isothermal assumption in the following.

4. Parametric analyses

In order to highlight how the previous results can be influenced by either the volume, the duct diameter, the importance in the amount of change in the boundary conditions (the pressure step's value) and its dynamic (slope to reach the step's value), several simulations have been performed and are presented in the following. These enable to introduce the value of developing a dimensionless analytical approach.

Two sub-sections are presented below for the analyses of geometry characteristics in a first part and boundary conditions in a second part.

4.1. Geometry analyses

Except if specified otherwise, the reference case will refer to the case above with a volume of 5 × 5x5m^3, 0.2 m duct's diameter for both ducts.

Volume and diameter impacts are analyzed through three different building types that can correspond to real cases of application: the dwelling's scale, the industrial hall's scale and the entertainment hall's

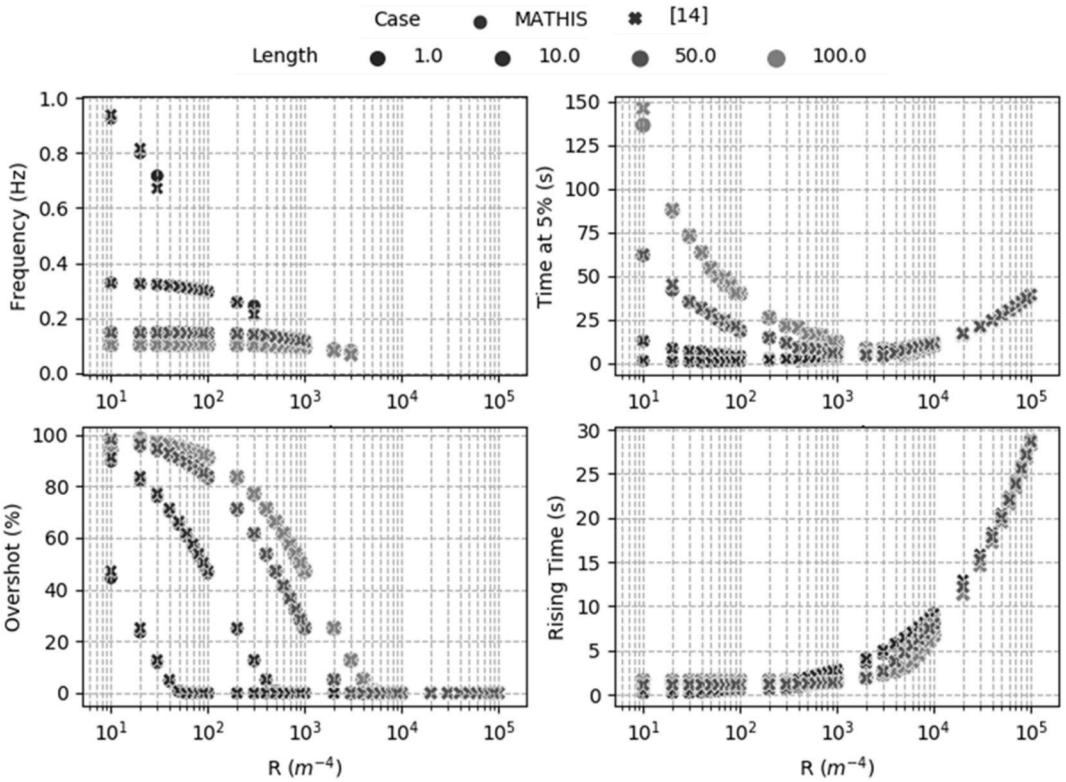

Fig. 4. Internal pressure resonance indicators for several duct's length (m) and resistance. Reference's results from Ref. [14] and MATHIS' results.

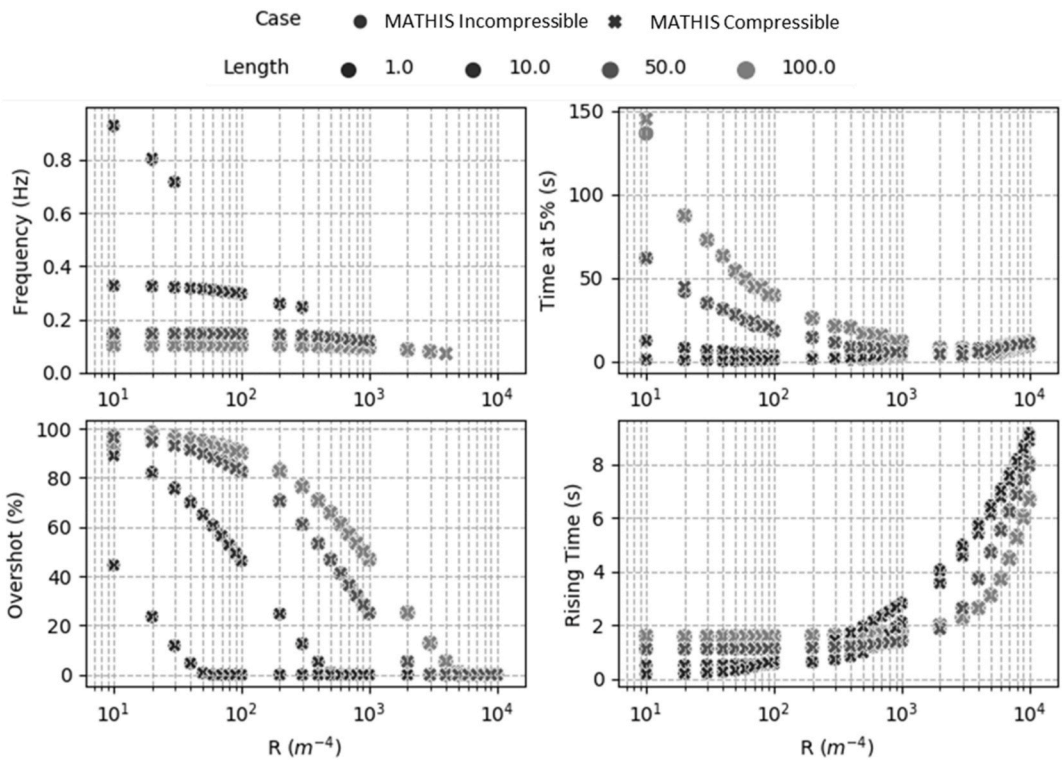

Fig. 5. Internal pressure resonance indicators for several duct's length (m) and resistance with compressible flow and incompressible flow.

scale. For all cases, only a duct length of 1 m is considered as it can be seen as a reference value for generic applications and it should enable to distinguish the different effects as, from the previous figures, the highest frequencies were obtained with the smallest inertia. The dwelling has the same opening as the reference case but with bigger volume of 250 m^3. The industrial hall's scale is characterized by a large volume of 100 $\times$ 100 m^2 of floor area with a ceiling of 10 m high, while the dwelling is represented by a floor area of 10 $\times$ 10 m^2 and a ceiling high of 2.5 m. Thus the industrial hall's scale has a diameter of 4 m and the dwelling's scale has a diameter of 0.2 m. The entertainment hall's scale has dimensions gathered from a real theater in Paris (the OLYMPIA) which has a floor area of 855 m^2 and a ceiling high of 13.3 m. The diameter used for this case is 2.54 m as it represents approximately the cumulative airflow paths' section of the theater. Using such an approach still leads to diminish global inertia. As said previously, the 1 m length enables to keep the generic approach wanted in these simulations. For each model, parametric simulation is carried on varying the duct's aeraulic resistance.

The results are plotted with the reference case in Fig. 6. For the sake of simplicity, only the frequency and the overshoot are presented.

From Fig. 6, one can notice that the industrial and dwelling's scales have identical results. The oscillation frequency is inversely proportional to the product of the duct's inertia and the zone's internal volume [2], which is similar for these two cases. Thus, the results obtained for these two cases, in terms of both frequency and overshoot are very close and can be seen as identical.

Then, the theater's scale presents the higher frequencies while the two others (industrial hall and dwelling's scales) present the lowest ones. These are to be explained, here again, by the product of the zone's internal volume and the duct's inertia that is lower for the theater's scale than for all other cases, leading to higher frequency observations.

The overshoot observed for the different cases shows that amplitudes of oscillations are stronger for the theater's scale than the other cases. It is worth noticing that it also has the highest inertia compared to the others diameter. Similar trends were obtained from Ref. [14].

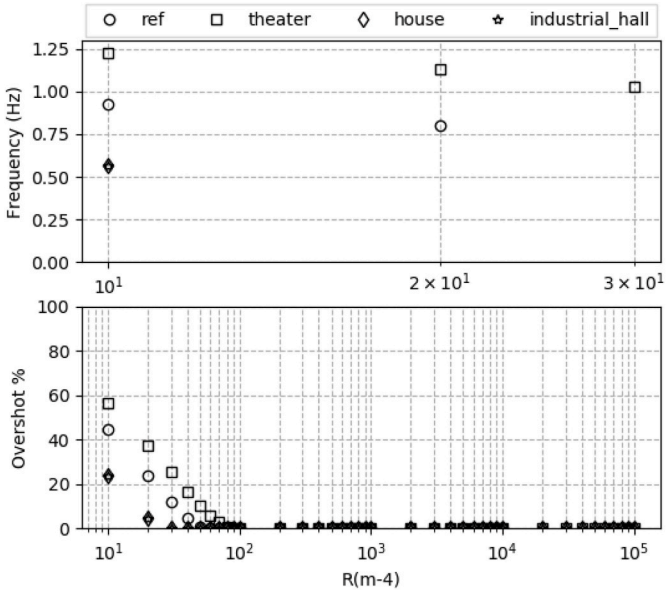

Fig. 6. Difference of frequency using 1 m duct between several configurations.

4.2. Boundary conditions analyses

In this sub-section, the boundary conditions characteristics are analyzed further changing the pressure step's size and its dynamics.

In the following, the reference's case is kept but the pressure step is changed to represent different wind bursts. As 2000 Pa represents quite an unrealistic wind burst of 57 m/s (but still realistic for an industrial vacuum vessel bursting's accident), it is lowered down in pressure to represent up to small wind's variation to represent down to a 1 m/s pressure step. Same approach is realized as previously, with parametric simulation for each boundary conditions and changing the duct's

aeraulic resistance.

Fig. 7 shows the frequency and the overshoot for the referenced case with several pressure's steps presented through wind velocities steps of 57 m/s (reference's case), 30 m/s, 5 m/s and 1 m/s.

From Fig. 7, one can observe the same threshold of frequency for lower duct's resistance. The frequency then decreases with increasing the duct's resistance as already seen in previous figures. This is explained by the balance between the inertia and the resistance of the duct in the mechanical energy balance given in equation (5). It is worth noticing that for lower pressure steps, the oscillation occurs for higher duct's resistances. Indeed, for the lowest pressure value, the frequency starts to decrease for duct resistance above 10 000 m^{-4} while the same trend is observed at $10m^{-4}$ for the 30 m/s step. Concerning the overshoot (amplitude), the lower the pressure step the higher the amplitude obtained. Even though this could be counter intuitive, it shall be recalled that the overshoot is expressed in relative value and can thus be in fact of quite small amplitude in absolute values. Nevertheless, oscillations still occur with a greater relative amplitude for the lower pressure steps.

The above analyses were made considering instantaneous pressure steps. In order to consider more realistic boundary conditions' perturbation, the impact of the slope of the pressure step is analyzed. The different studied slopes are represented in Fig. 8.

Varying the pressure step's slope consists in having the same pressure step with linear increasing pressure up the final value in 0.5 s, 1 s and 2 s. Results are compared to the reference's case with instantaneous variation (0.005 s as the simulation's time step). Fig. 9 shows, as previously, only the frequency and the oscillation's amplitude through the overshoot.

From Fig. 9, no oscillation is observed for slopes abos 1s even if small overshot still occur. Besides, the frequency obtain form the instantaneous step and a slop of 0.5 s remain the same for small aeraulic resistance (on value obtained with R = 10 m^{-4}). Indeed as it depends on the product of the inertia with the internal volume, there is no reason it should be influenced by the boundary condition step's slope. On the contrary, the overshoot is greatly influenced as seen in Fig. 9's lower graph. The obtained results are intuitive here as the greater the slope, the more time the system has to reach the stabilized regime and thus small amplitudes are observed. From all figures presented in the parameters analyses section, it seems that the assumption of quasi-staticity cannot be valid for most of the cases and in particular for small disturbances that are more likely to happen in real applications. Besides, from all the trends observed on the different indicators, a quite identical evolution is noticed, thus implying that dimensionless ratios could be defined for any cases.

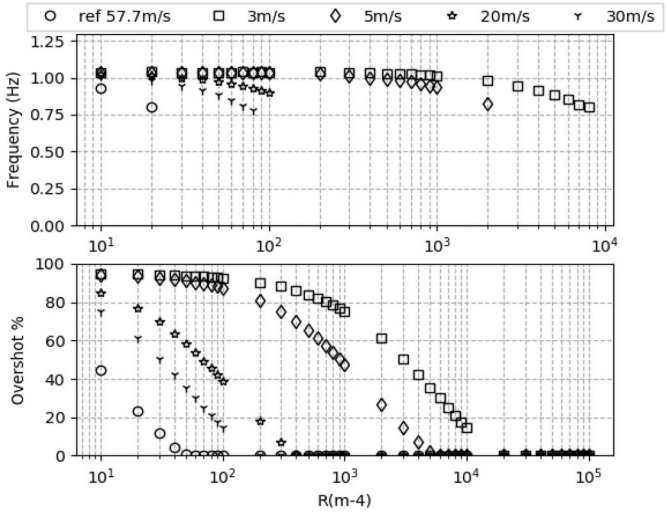

Fig. 7. Difference of frequency using 1 m duct between several velocities.

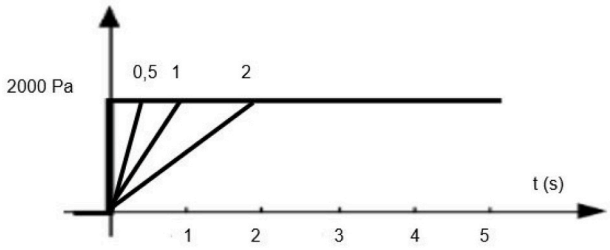

Fig. 8. Slope variation (0,5-1-2 s).

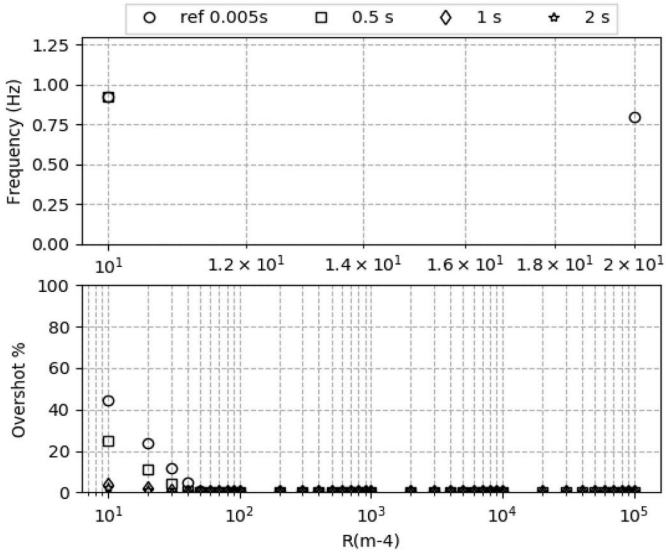

Fig. 9. Difference of frequency using 1 m duct between several ramps.

This dimensionless approach is presented in the following sections.

5. Dimensionless analysis

The dimensionless approach consists in considering reference's scales for each physical variable in order to build dimensionless balances for the first physical balanced equations.

The mechanical energy balance for a branch, considering isothermal condition, is presented by the generalized Bernoulli's equation written in equation (5). Considering the volume flow rate and the aeraulic resistance value explicitly in the same equation leads to expression (9).

$$\frac{L\rho \mathrm{d}Q}{S\mathrm{d}t} = \Delta P + R\rho(Q)^2 \tag{9}$$

The mass balance in the internal node, under these assumptions, is expressed by expression (10):

$$\frac{d\rho V}{\mathrm{dt}} = \sum_{\mathrm{i}} \rho \mathrm{Q_i} + \sum_{\mathrm{j}} \rho \mathrm{Q_j} \tag{10}$$

LeRoux in Ref. [14] established his dimensionless model from the same equations as above, say the mechanical energy balance and the mass balance. The referenced values for each physical variable used to establish the dimensionless model are presented in Table 1.

Thus using the dimensionless variables into equations (9) and (10) above leads to the following dimensionless balances for the mechanical energy (11) and the mass conservation (12).

$$\frac{\rho^* L^*}{S^*}\frac{dQ^*}{dt^*} = \Delta P^* - \left(R_{ref} S_{ref}^2\right)\rho^* R^* Q^{*2} \tag{11}$$

Table 1
Table of dimensionless variable.

Reference Variable	Dimensionless variable
V_{ref}	$V^* = V/V_{ref}$
L_{ref}	$L^* = L/L_{ref}$
S_{ref}	$S^* = S/S_{ref}$
ρ_{ref}	$\rho^* = \rho/\rho_{ref}$
U_{ref}	$U^* = U/U_{ref}$
$P_{ref} = \rho_{ref} * U^2_{ref}$	$P^* = P/\rho_{ref} * U^2_{ref}$
$Q_{ref} = S_{ref} * U_{ref}$	$Q^* = Q/S_{ref} * U_{ref}$
R_{ref}	$R^* = R/R_{ref}$
$t_{ref} = L_{ref}/U_{ref}$	$t^* = t/L_{ref}/U_{ref}$

$$\frac{dP^*}{dt^*} = \left(\frac{P_{atm} S_{ref} L_{ref}}{\rho_{ref} U^2_{ref} V_{ref}}\right)\left(\frac{\sum_i \rho^* Q^*_i + \sum_j \rho^* Q^*_j}{V^*}\right) \tag{12}$$

The above expressions give two dimensionless groups of variables which describe the new system of mechanical energy balance and mass conservation. These two groups are given in expressions (13) and (14).

$$A_1 = R_{ref} S^2_{ref} \tag{13}$$

$$A_2 = \frac{P_{atm} S_{ref} L_{ref}}{\rho_{ref} U^2_{ref} V_{ref}} \tag{14}$$

These two terms explain the physical ratio involved in such system. Dimensionless analyses are interesting to highlight general trends for any dimension considered in the system. Thus, reduced scale experiments can be conducted keeping these ratios identical whatever the scale of analysis is. As introduced earlier, from the parametric simulation, similar curve patterns were obtained for the different cases, but finding the correct groups of terms that would make the overall cases follow the same curve is not strait forward. A coupled process of analyses and attempt is realized in the present case.

A first step is introduced through the different obtained in Fig. 7. Indeed, from Fig. 7, the frequency's threshold depends on both the input pressure step value and the aeraulic resistance. Indeed, the aeraulic resistance's threshold decreases as the input pressure step increases. Thus, the product of both, by considering the ratio of the two dimensionless groups defined earlier, is to be considered. This would lead to the representation of the same cases in terms of the frequency in the y axis and the ratio of both dimensionless term A1 and A2 along the x-axis, proposed in Fig. 10.

Fig. 10 highlights that the ratio of A1 over A2 can make the different cases be merge into one trend. But this first step was possible because of the frequencies over the different cases.

The main variable of interest is the resonance frequency computed out of the internal pressure fluctuation along time. As the Strouhal number is generally considered for time dependent analysis of regular patterns, the second step consists of finding which element would have to be introduced in order make all the different cases converge into one single trend. The Strouhal Number is defined by the product of the frequency with a referenced length over a referenced velocity. Thus, when the frequency is computed out of the pressure signal, it should be multiplied by the ratio the referenced length over the referenced velocity. Between the two dimensionless groups introduced earlier, A2 contains the above-mentioned ratio of length over velocity and contains other referenced ratios given from making the conservation of mass being dimensionless. It should be thus introduced as well. The following expressions present the Strouhal number definition (16), the way to introduce A2 in the new expression (16) and finally the factor used to multiply the computed frequency in order to compute the ratio of the Strouhal number over A2 (17).

$$St = f\frac{L_{ref}}{U_{ref}} \tag{15}$$

$$\sqrt{A_2} = \frac{L_{ref}}{U_{ref}}\sqrt{\frac{P_{atm} S_{ref}}{\rho_{ref} V_{ref} L_{ref}}} \tag{16}$$

$$\frac{St}{\sqrt{A_2}} = f\sqrt{\frac{\rho_{ref} V_{ref} L_{ref}}{P_{atm} S_{ref}}} \tag{17}$$

The previous cases were thus represented in Fig. 11, in terms of this new dimensionless parameters: the Strouhal number over the root square of A2 for the y-axis, keeping the above defined ratio of A1 over A2 for the x-axis.

Fig. 11 shows that by using the two dimensionless terms most of cases can be merge into one trend, but some cases still stand outside the others. So, a third step needs to be introduced.

The two 'outliers' are the industrial hall and the theater which have different ducts sections. This observation makes to integrate this difference into a new x-axis variable by dividing the above consider ratio of A1 above A2 by the square of the referenced section.

This attempt enables to merge all the different cases into one single trend as shown in Fig. 12. Other configurations are also added in Fig. 12 in order to validate the unique trend for all cases.

The rearrangements were made with the will to make possible a unique representation of all the different cases. This aim was reached with the introduction of the square of the referenced section into T_x

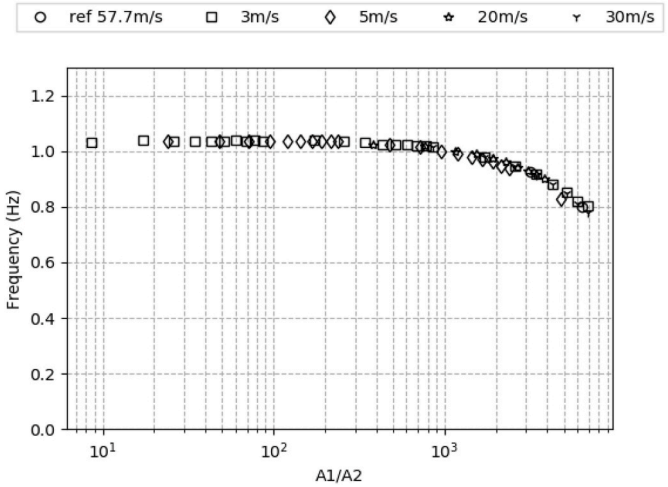

Fig. 10. Regrouping velocity frequency in function of A1/A2 term in x-axis.

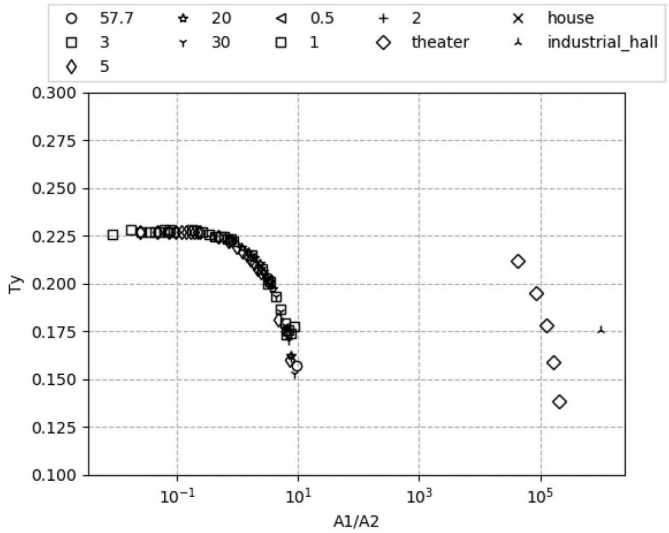

Fig. 11. Internal fluctuation for all cases in function of non-dimensional terms.

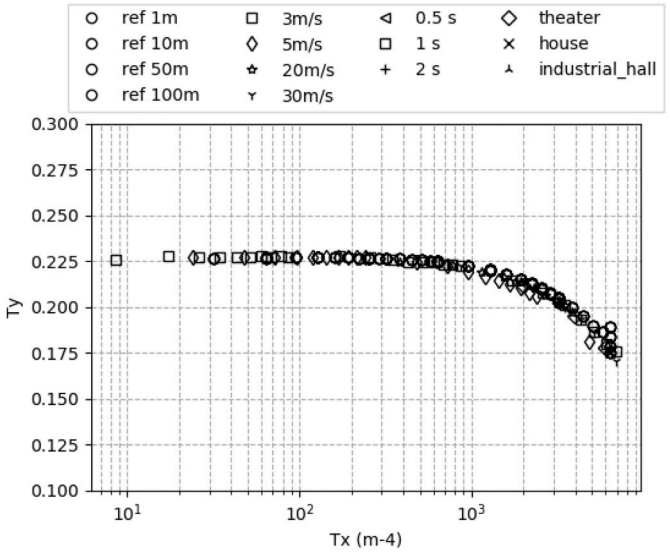

Fig. 12. Generalization of Frequency Plots.

which makes this last no more dimensionless. Nevertheless, the group T_y introduced the Strouhal number and T_x enabled to merely merge all the cases into one trend.

$$T_x = \frac{R_{ref} V_{ref} P_{ref}}{P_{atm} S_{ref} L_{ref}} = \frac{A_1}{A_2 * S_{ref}^2} \tag{18}$$

$$T_y = \frac{f\sqrt{\rho_{ref} V_{ref} L_{ref}}}{\sqrt{P_{atm} S_{ref}}} = \frac{Strouhal}{\sqrt{A_2}} \tag{19}$$

Using such global results, Fig. 12 shows that in case of a T_x value above 10 000 m^{-4}, no frequency would be detected and therefore no pressure fluctuation inside the zone leading to the validity of the quasi-static assumption. Below this value, the quasi-static assumption is not valid: lower time steps and non-stationarity caution should be considered while simulating ventilation systems. As a reminder the reference case is the isotherm and incompressible case with Mathis. Such results, graphically represented as one single curve, can be very useful for one who would investigate whether the quasi-static assumption should be kept. These conclusions are steered by rigorous analyses of any possible internal pressure fluctuation. But, as said earlier, the overshoot is computed in a relative form, thus, even though some oscillations could be observed these could also remain in very small absolute without significant errors for engineering application. Thus, in these cases, the quasi-static assumption could still be considered.

The advantage of this graph is that it allows to easily detect the frequency of any system and get an idea about the value of the internal fluctuation. Finally, as an example of use: if one has a theater to design with a volume of 11371 m^3 and a duct where (L = 1 m, D = 2.42 m and resistance of 10 m^{-4}); taking a wind velocity of 10 m/s for a quite small storm event, a value of 29.9 will be computed for T_x. The intersection with the graph gives T_y = 0.223, which, for this example, leads to a frequency of 1.29 Hz. The first advice would be to avoid the quasi-static assumption in order to catch the maximum amplitude that could occur. The following simulations, using adequate software and assumption will afterward enable to define if inertia can finally be neglected in the system. If the oscillation's amplitudes are small and are not to raise a structure or comfort issue, the designing process can go on using faster simulation by considering the quasi-static assumption.

6. Conclusion

In this study, the MATHIS software is used to analyze, through parametric simulation on a simple case, the internal pressure fluctuation under several pressure steps of boundary conditions. After MATHIS being validated under non-stationary conditions, it was used to simulate several cases, changing either the geometric parameters, the ducts' pressure characteristics, the zone volume and the ramp slope of the increasing boundary conditions (from instantaneous up to 2 s).

Results are analyzed in a dimensionless form in order to merge all the cases under two unique groups of variables. These two groups enable to highlight if a fluctuation can be present and to compute the frequency of the pressure's fluctuation for a set of parameters. From the results obtained with the different cases, the assumption of quasi-staticity does not seem to be valid for the consideration of dynamic fluctuation of the boundary conditions created by the wind for example.

These two main expressions are computed from an analysis on the single zone configuration with two openings through ducts (thus considering inertia effect compared to sharped openings). For configuration with more than one zone, the two above expressions are still accurate by considering one zone after the other. The consideration of several zones included in one analysis will damper the resonance effect in each zone by adding resistance in the overall network. The zones in direct contact to the pressure steps being studied (either from external boundary conditions or from internal accidental events) can be subject to resonance effect and will lower down the effect to the other zones through the air flow paths resistance between each.

Thus, studying the resilience of ventilation systems to either wind turbulence, or any other sudden changes in the boundary condition should consider the duct's inertia, and compute the potential internal pressure resonance event. Decision can be taken afterward to neglect these effects if the overshoot remain below some threshold to be defined for each specific case.

CRediT authorship contribution statement

Ali Esber: Writing – review & editing, Writing – original draft, Validation, Methodology, Formal analysis, Data curation. **Xavier Faure:** Methodology, Supervision, Validation, Writing – review & editing. **François Demouge:** Writing – review & editing, Validation, Supervision, Methodology. **Etienne Wurtz:** Methodology, Project administration, Supervision, Validation. **Simon Rouchier:** Writing – review & editing, Validation, Supervision.

Declaration of competing interest

The authors declare that they have no known competing financial interests or personal relationships that could have appeared to influence the work reported in this paper.

Acknowledgement

The presented study is a part of a global project which aims to study the aerodynamic effects induced by external wind on the overall performance of ventilation systems (energy, air quality, humidity).

This work and the research behind it would not have been possible without the exceptional support of my supervisors, directors and all the team of my institutes who collaborate (CEA, CSTB and USMB).

References

[1] X. Faure, F. Losfeld, I. Pollet, E. Wurtz, O. Ouvrier Bonnaz, Resilient demand control ventilation system for dwellings, in: 39th AIVC Conference, Jun Les Pins, FRANCE, 2018.

[2] J.D. Holmes, Mean and fluctuating internal pressures induced by wind, July 1979, in: Proceedings, 5th International Conference on Wind Engineering, Fort Collins, 1979. IV-8-1.

[3] F. Haghighat, J. Rao, P. Fazio, The influence of turbulent wind on air change rates and modelling approach, Build. Environ. 26 (2) (1991), 95±109.

[4] J.H. Oh, G.A. Kopp, D.R. Inculet, The UWO contribution to the NIST aerodynamics database for wind loads on low buildings: part 3, Inter. Press. J. Wind. Eng. Ind. Aerodyn. 95 (2007) 755–779.

[5] B.J. Vickery, C. Bloxham, Internal pressure dynamics with a dominant opening, J. Wind Eng. Ind. Aerod. 41–44 (1992) 193–204.
[6] A.R. Woods, P.A. Blackmore, The effect of dominant openings and porosity on internal pressures, J. Wind Eng. Ind. Aerod. 57 (1995) 167–177.
[7] W. Pearce, D.M. Sykes, Wind tunnel measurements of cavity pressure dynamics in a low-rise flexible roofed building, J. Wind Eng. Ind. Aerod. 82 (1999) 27–48.
[8] T.C.E. Ho, D. Surry, D. Morrish, G.A. Kopp, The UWO contribution to the NIST aerodynamic database for wind loads on low buildings: part 1. Archiving format and basic aerodynamic data, J. Wind Eng. Ind. Aerod. 93 (2005) 1–30.
[9] D.W. Etheridge, Unsteady flow effects due to fluctuating wind pressures in natural ventilation design – mean flow rates, Build. Environ. 35 (2000) 111–133.
[10] D.W. Etheridge, Unsteady flow effects due to fluctuating wind pressures in natural ventilation design – instantaneous flow rates, Build. Environ. 35 (2000) 321–337.
[11] Mounajed La modélisation des transferts d'air dans les bâtiments. Application à l'étude de la ventilation, Ecole Nationale des Ponts et Chaussees, 1989.
[12] N. Le-Roux, Etude par similitude de l'influence du vent sur les transferts de masse dans les bâtiments complexes, PhD thesis, University of La Rochelle, 2011.
[13] Faure X. Le-Roux, C. Inard, S. Soares, L. Ricciardi, Reduced-scale study of wind influence on mean airflows inside buildings equipped with ventilation systems, Build. Environ. 58 (2012) 231–244.
[14] Le Roux, Inard Faure, Ricciardi Soares, Reduced-scale study of transient flows inside mechanically ventilated buildings subjected to wind and internal overpressure effects, Build. Environ. 62 (2013) 18–32.
[15] Demouge F, Mathis: Technical guide. Open-Source heat and mass transfer software, CSTB - Centre scientifique et technique du batiment, https://gitlab.com/CSTB/mathis/-/tree/master/.
[16] F. Demouge, N. Le Roux, et X. Faure, «Numerical Validation for Wind Driven Ventilation Design» 32nd AIVC Conference, 2011. Brussels.
[17] T. Clerc, F. et Demouge, «Evaluation of the Performance of the Thermal and Aeraulic Building Simulation Software MATHIS with the BESTest Method, » CSTB, EN-CAPE 16.148 R-V0, 2016.
[18] S. Mélis, P. Querre, L. Ricciardi, Physical Modeling of the SYLVIA Code, IRSN, 2008-02.